ISBN: 978-3-95450-231-8 ISSN: 2673-5490 doi: 10.18429/JACoW-IPAC2023-WEPL161

STABILITY SURVEY OF A DOUBLE RF SYSTEM WITH RF FEEDBACK LOOPS FOR BUNCH LENGTHENING IN A LOW-EMITTANCE SYNCHROTRON RING

N. Yamamoto*, T. Yamaguchi, KEK, Tsukuba, Ibaraki, Japan
P. Marchand, A. Gamelin, R. Nagaoka, Synchrotron SOLEIL, Gif-sur-Yvette, France

Abstract

Bunch lengthening with a double radio-frequency (rf) system combining fundamental and harmonic cavities (HC) is essential in achieving extremely low emittance along with suitable lifetime, as required for ring-based fourth-generation synchrotron radiation light sources in the low-to-medium energy range. For this purpose, we are investigating the use of a powered HC, so-called "active HC". Its advantage, as compared to the more commonly used "passive HC", is the possibility of preventing some beam instabilities by proper control of the rf external generator. In this paper, the impact of a direct rf feedback on the unstable beam motion at the vicinity of the "flat-potential" condition is evaluated by particle tracking simulations for the SOLEIL II high current multi-bunch operation mode at 500 mA.

INTRODUCTION

Recent studies of double rf systems combining fundamental cavities (MC) and HC for bunch lengthening have pointed out that, in many cases, an unstable beam motion, as so-called "periodic transient beam loading (PTBL) effect" [1] or "coupled bunch mode $l = 1$ instability" [2], prevents from reaching the optimum bunch lengthening condition with high beam current. One effective way of pushing back such a bunch lengthening limit is to reduce the total R/Q of the HC. However, there is also a limit to the reduction of their R/Q due to the need for generating sufficient HC voltage for bunch lengthening.

We have then considered using an active (powered) HC with conventional rf feedback loops of two types, mode damper [3, 4] and direct rf feedback (DRFB) [5]. In our previous study in Ref. [4], the feasibility of an active HC system for bunch lengthening without any DRFB was numerically investigated for SOLEIL II by using the particle tracking code, mbtrack [6]. For the high current multi-bunch operation mode at 500 mA, the maximum stable bunch lengthening factor (BLF) of about 4 was obtained by using a single 2-cell 1.41 GHz cavity (HC), as developed at the ESRF [7], combined with four ESRF-EBS type 352 MHz cavities (MC) [8, 9]. The assumed machine and cavity parameters are listed in Tables 1 and 2 below.

In the above case, an unstable beam motion with bunch length fluctuations and an energy spread increase prevented from reaching the maximum BLF of 4.7, as predicted by the rf potential analysis [10]. At the instability threshold, the voltage slope factor ξ, defined by Eq. (3) of Ref. [4] or Eq. (3) of this paper was 0.972, and the amplification factor η, given by Eq. (22) in Ref. [11], was around 1.0, suggesting the occurrence of a PTBL instability.

In this paper, the impact on the PTBL instability of a DRFB loop, applied to the HC, is evaluated by using the particle tracking code, mbtrack2, which is an improved version of mbtrack, written in Python instead of C-code [12].

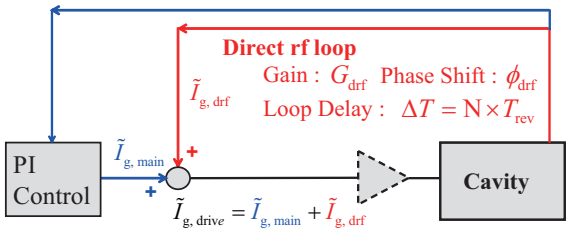

Figure 1: Schematic of the rf feedback system model used in the mbtrack2 code with DRFB (red) and PI controls (blue). The dashed triangle represents an rf amplifier, but it is not modeled in the mbtrack2 code.

DIRECT RF FEEDBACK

The DRFB loop is generally used in the MC rf control system as a countermeasure against the zero mode Robinson instability [5, 13]. By picking up a sample of the cavity voltage and adding it to the rf drive signal with proper gain and phase, one can reduce the cavity impedance as seen by the beam.

The rf control system modeled in mbtrack2 consists of Proportional-Integral, PI (blue) and DRFB (red) loops, as shown in Fig. 1. The "slow" PI loop is used conventionally to keep the cavity voltage constant at the specified value. In the "fast" DRFB loop, the rf signal, picked up at the cavity voltage $\tilde{V}_c$, is fed back to be added with the main rf generator current $\tilde{I}_{g,main}$[1]. In order to parameterize the DRFB loop, one introduces its gain G_{drf}, its phase shift ϕ_{drf} relative to $-\tilde{V}_c$ and its delay, $\Delta T = N \times T_{rev}$ (integer multiple of the ring revolution time).

The expected generator voltage component $\tilde{V}_{g,drf}$ induced by the DRFB loop is defined as follows :

$$\tilde{V}_{g,drf} = G_{drf}\tilde{V}_c \exp\{i(\psi - \phi_{drf})\}, \quad (1)$$

where ψ is the tuning angle of the cavity. Then the voltage is converted into generator current $\tilde{I}_{g,drf}$ by using the Eq. (25) in Ref. [14]. Once the drive generator current

* naotoy@post.kek.jp

[1] The notation $\tilde{X}$ indicates that the variable X is treated as a complex number.

ISBN: 978-3-95450-231-8 ISSN: 2673-5490 doi: 10.18429/JACoW-IPAC2023-WEPL161

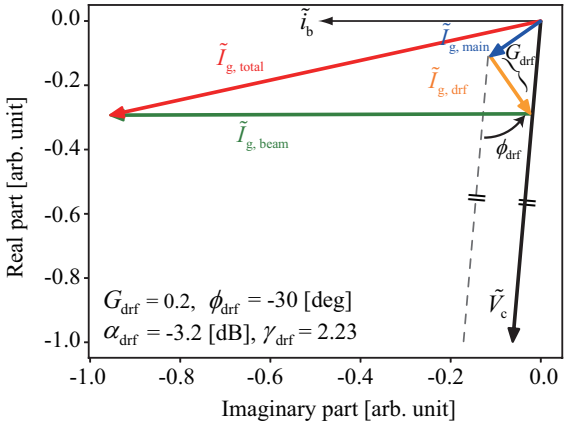

Figure 2: Typical phasor diagram of the DRFB loop for HC, indicating the total current $\tilde{I}_{g,total}$, DRFB current $\tilde{I}_{g,drf}$, main (PI loop) current $\tilde{I}_{g,main}$ and beam current $\tilde{I}_{g,beam}$. Each phasor is normalized to $|\tilde{V}_c|$.

$\tilde{I}_{g,drive} = \tilde{I}_{g,main} + \tilde{I}_{g,drf}$ is obtained, it is re-converted to the total generator current induced in the cavity by using the Eq. (26) in Ref. [14]. The PI loop controls $\tilde{I}_{g,main}$ to keep $\tilde{V}_c$ at the set value.

For the purpose of quantifying the performance of the DRFB loop in the whole system, the amplitude ratio α_{drf} and gain γ_{drf} are introduced as follows :

$$\alpha_{drf} = |\tilde{I}_{g,drf}/\tilde{I}_{g,drive}|, \gamma_{drf} = \alpha_{drf}/(1-\alpha_{drf}). \quad (2)$$

These definitions are the same as in Ref. [5] and α_{drf} is often represented in dB units.

A typical phasor diagram of the DRFB loop for HC is shown in Fig. 2. Each phasor is normalized to $|\tilde{V}_c|$. The parameter set corresponds to the case shown in Fig. 4 at (G_{drf},ϕ_{drf})=(0.2,-30) and α_{drf} is estimated to be -3.2 dB.

INVESTIGATION SETUP

As in the previous study [4], the investigation has been carried out for the SOLEIL-II v0356 lattice[15] and the double RF system, whose parameters are listed in Tables 1 and 2. It is assumed that both types of cavities, MC and HC, are "HOM free"

The mbtrack2 simulations are performed in one-dimension (longitudinal) and both MC and HC fundamental impedance's are considered as instability sources. The DRFB loop is applied only to the HC. For each cavity, the parameter set is determined in advance to provide the specified cavity voltage and phase under the beam loading of a point-charge located at the synchronous phase, which minimize the required generator power for both MC and HC.

Table 1: SOLEIL-II Parameters (v0356)

Parameter	Unit	Value
Energy	GeV	2.75
RF frequency	MHz	351.6
Energy loss per turn	keV	458
Main RF voltage	MV	1.80
Energy spread		8.8×10^{-4}
Momentum compaction factor		1.05×10^{-4}
Longitudinal damping time	ms	12.2
Natural rms bunch length	ps	8.5

Table 2: Cavity Parameters of the Double RF System

Parameter	MC	HC (2 cell)
Harmonic number	1	4
Shunt Impedance, $R_s = V_c^2/2P_c$	5.0 MΩ	2.4 MΩ
Unloaded-Q	35000	27000
Cavity coupling coefficient	5.0	1.0
Cavity number	4	1

For the HC, during the tracking simulation, especially for the early turns, $\tilde{V}_c^{HC}$ and $\tilde{I}_{g,drf}^{HC}$ vary as the bunch distribution and phase change until the steady-state condition is reached. Both ψ_{HC} and $\tilde{I}_{g,main}^{HC}$ are treated as constant during the tracking simulation. In the mean time, for the MC, ψ_{MC} and $\tilde{I}_{g,main}^{MC}$ are slowly changed to achieve the specified $\tilde{V}_c^{MC}$ with the accuracy of 1×10^{-3}. The feedback variables of the rf system are updated at a frequency of 1.63 MHz, which is around twice the ring revolution frequency.

Practically, ΔT of about 1 μs is expected, but for the sake of clarity, it is assumed to be zero. In the case of non-zero ΔT, the stable ranges of the feedback parameters, G_{drf} and ϕ_{drf}, are limited. However, as far as G_{drf} and ϕ_{drf} are kept within these limits, the stability of the whole system should not be affected.

In the calculations reported here, the number of macro particles per bunch is set to 1000 in order to reduce the computation time. This is acceptable for evaluating the effect of the DRFB loop, however may be insufficient to precisely evaluate the achievable bunch length. Therefore, for evaluating the bunch lengthening efficiency, one uses, instead of the bunch length, the parameter ξ at the stable steady-state condition, which is given by :

$$\xi = -4\,\mathrm{Im}\,\tilde{V}_c^{HC}/\,\mathrm{Im}\,\tilde{V}_c^{MC}. \quad (3)$$

A detailed discussion about the achievable bunch lengths shall be provided in another paper.

CALCULATION RESULT

From the rf potential analysis, assuming $|\tilde{V}_c^{MC}|$=1.80 MV, the flat potential (FP) condition, that is ξ=1.0, is met when $|\tilde{V}_c^{HC}|$=434 kV, ψ_{HC} ≅138.2 kHz with minimum required generator power. This case is illustrated in Fig. 3 showing the coupled-bunch [4] and PTBL [11] instability thresholds. It is found that the PTBL threshold curve (pink) crosses the HC R_s line (dark-orange) at ψ_{HC} ≅138.2 kHz.

As a result of mbtrack2 simulations with 500 mA in uniform filling, instabilities are observed when $|\tilde{V}_c^{HC}|$>425 kV, ψ_{HC}<141 kHz, ξ>0.976 and η>0.998. Then, the impact of G_{drf} and ϕ_{drf} on the beam motion is investigated slightly

ISBN: 978-3-95450-231-8 ISSN: 2673-5490 doi: 10.18429/JACoW-IPAC2023-WEPL161

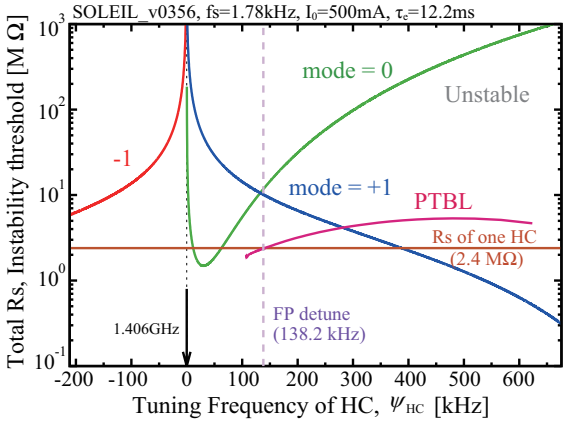

Figure 3: HC R_s threshold for instabilities, taking into account the MC R_s and the parameters in Table. 1. The threshold plots for PTBL (pink) and coupled-bunch instabilities, modes : -1 (red), 0 (green) and 1 (blue). Unstable beam motions are expected above each threshold curve.

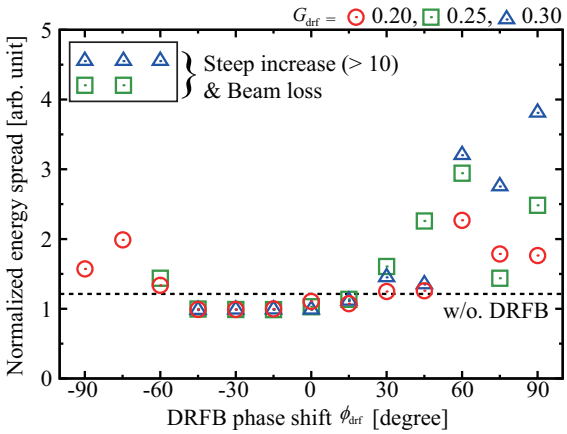

Figure 4: Energy spread divided by the natural one over the bunch train versus ϕ_{drf}, for G_{drf}=0.2 (red circles), 0.25 (green squares) and 0.3 (blue triangles). The energy spread without DRFB loop is also indicated by a dashed black line.

above this threshold, at ψ_{HC}=138.6 kHz and η=1.011. At this parameter set, without the DRFB loop, the unstable beam motion is observed, and the energy spread increases from the natural value of 8.9 $\times 10^{-4}$ to 1.08 $\times 10^{-3}$.

In Fig. 4, as an indicator of the beam stability, the normalised energy spread at 60 k-turns is plotted versus ϕ_{drf} between -90 to 90° in step of 15°, for different values of G_{drf}, 0.20, 0.25 and 0.30. These plots suggest the existence of some stabilising effect from the DRFB loop for ϕ_{drf} between 15 and -45° and full stabilisation with normalised energy spread equal to one for ϕ_{drf} between -15 and -45°. As an example, the periodic modulations of the bunch length along the bunch train, which characterizes a PTBL instability, is shown in Fig. 5 for (G_{drf},ϕ_{drf})=(0.2,90).

The phasor diagram shown in Fig. 2 corresponds to the case (G_{drf},ϕ_{drf})=(0.2,-30). At this working point, the HC parameters are $|\tilde{V}_{\mathrm{c}}^{\mathrm{HC}}|$=432 kV, ξ=0.994 and one finds that

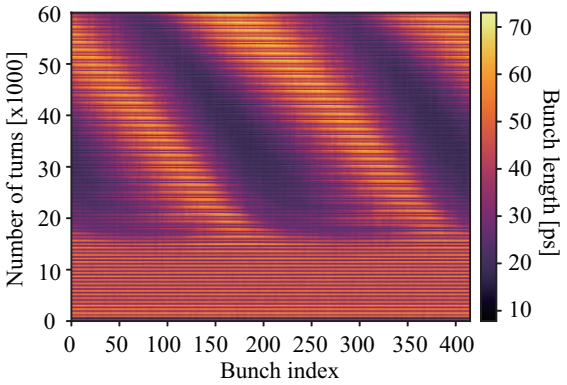

Figure 5: Evolution of the rms bunch length versus bunch index.

α_{drf}=-3.2 dB and γ_{drf}=2.23, which are considered to be reasonable values when compared with the experimental values reported in Ref. [5]. The generator power of the HC, calculated from $\tilde{I}_{\mathrm{g,drive}}$, is 26.4 kW, very close to the required 26.3 kW at the maximum voltage of 425 kV, which is achievable under stable conditions without DRFB loop.

With the DRFB loop set at (G_{drf},ϕ_{drf})=(0.3,-30), one can almost reach the FP condition (ξ=0.995). Further bunch lengthening is prevented by unstable beam motion with bunch length fluctuations along the bunch train. Although it is not detailed in this paper, similar calculations show that, thanks to the DRFB, one can operate under stable conditions at the FP condition with 100 mA in 8 bunches. Further investigations are required in order to evaluate more precisely the beneficial effect of the DRFB on the maximum achievable bunch lengthening.

SUMMARY

The impact on the beam stability of a DRFB loop, applied to the active HC of a double rf system (MC + HC) for bunch lengthening, was investigated using the particle tracking code mbtrack2.

For the SOLEIL-II high current multi-bunch operation mode at 500 mA, one finds that a DRFB loop can help to push back the PTBL instability threshold at the vicinity of the FP condition, which should allow to reach longer bunch lengths without significant increase of the generator power.

However, further understanding of the theoretical aspects and systematic studies under various conditions are necessary for a more precise evaluation of the beneficial effect of the DRFB loop on the maximum achievable bunch length.

ACKNOWLEDGEMENTS

This work was supported by JSPS KAKENHI Grant Number JP20H04459. It has been accomplished as part of a RF collaboration between different labs (KEK, PSI, ESRF, BESSY and SOLEIL). We thank our partners for the useful exchanges.

ISBN: 978-3-95450-231-8 ISSN: 2673-5490 doi: 10.18429/JACoW-IPAC2023-WEPL161

REFERENCES

[1] T. He *et al.*, "Periodic transient beam loading effect with passive harmonic cavities in electron storage rings," *Phys. Rev. Accel. Beams*, vol. 25, paper 024401, 2 2022. doi:10.1103/PhysRevAccelBeams.25.024401

[2] M. Venturini, "Passive higher-harmonic rf cavities with general settings and multibunch instabilities in electron storage rings," *Phys. Rev. Accel. Beams*, vol. 21, paper 114404, 11 2018. doi:10.1103/PhysRevAccelBeams.21.114404

[3] K. Hirosawa *et al.*, "Development of a Longitudinal Feedback System for Coupled Bunch Instabilities Caused by the Accelerating Mode at Superkekb," in *Proc. IPAC'17*, Copenhagen, Denmark, May 2017, pp. 3989–3991. doi:10.18429/JACoW-IPAC2017-THPAB115

[4] N. Yamamoto, S. Sakanaka, P. Marchand, P. Gamelin, and R. Nagaoka, "Feasibility study of an active harmonic cavity for bunch lengthening in an electron storage ring," in *Proc. of the 19th Annual Meeting of Particle Accelerator Society of Japan*, 2022, paper WEP059. http://www.pasj.jp/web_publish/pasj2022/proceedings/PDF/WEP0/WEP059.pdf

[5] K. Akai, "Stability analysis of rf accelerating mode with feedback loops under heavy beam loading in superKEKB," *Phys. Rev. Accel. Beams*, vol. 25, paper 102002, 10 2022. doi:10.1103/PhysRevAccelBeams.25.102002

[6] N. Yamamoto, A. Gamelin, and R. Nagaoka, "Investigation of Longitudinal Beam Dynamics With Harmonic Cavities by Using the Code Mbtrack," in *Proc. IPAC'19*, Melbourne, Australia, May 2019, pp. 178–180. doi:10.18429/JACoW-IPAC2019-MOPGW039

[7] A. D'ELia *et al.*, "Design status of a 4th harmonic cavity for ESRF-EBS," *presented at 25th ESLS RF Meeting*, 2021.

[8] J. Jacob, P. B. Borowiec, A. D'Elia, G. Gautier, and V. Serrière, "ESRF-EBS 352.37 MHz Radio Frequency System," in *Proc. IPAC'21*, Campinas, Brazil, May 2021, pp. 395–398. doi:10.18429/JACoW-IPAC2021-MOPAB108

[9] A. D'Elia, J. Jacob, and V. Serrière, "ESRF-EBS 352 MHz HOM Damped RF Cavities," in *Proc. IPAC'21*, Campinas, Brazil, May 2021, pp. 1034–1036. doi:10.18429/JACoW-IPAC2021-MOPAB333

[10] A. Hofmann and S. Myers, "Beam dynamics in a double rf system," CERN-ISR-TH-RF-80-26, 1980, pp. 610–614.

[11] T. He, "Novel perturbation method for judging the stability of the equilibrium solution in the presence of passive harmonic cavities," *Phys. Rev. Accel. Beams*, vol. 25, paper 094402, 9 2022. doi:10.1103/PhysRevAccelBeams.25.094402

[12] A. Gamelin, W. Foosang, and R. Nagaoka, "Mbtrack2, a collective effect library in python," in *Proc. IPAC2021*, 2021, pp. 282–285. doi:10.18429/JACoW-IPAC2021-MOPAB070

[13] P. Marchand *et al.*, "Operation of the SOLEIL RF system," in *Proceedings of PAC07*, 2007, pp. 2050–2052. https://accelconf.web.cern.ch/p07/PAPERS/WEPMN004.PDF

[14] N. Yamamoto *et al.*, "Reduction and compensation of the transient beam loading effect in a double rf system of synchrotron light sources," *Phys. Rev. Accel. Beams*, vol. 21, paper 012001, 1 2018. doi:10.1103/PhysRevAccelBeams.21.012001

[15] A. Loulergue *et al.*, "TDR Baseline Lattice for the Upgrade of SOLEIL," in *Proc. IPAC'22*, Bangkok, Thailand, 2022, pp. 1393–1396. doi:10.18429/JACoW-IPAC2022-TUPOMS004